# Not so smooth after all: resolving dust and gas structures in protoplanetary disks

Cazzoletti, P.

# 1 Introduction

One of the most fascinating astronomical achievements of all times has been the discovery in the last couple of decades of planets outside of the Solar System, called "exoplanets", orbiting stars other than our own Sun. Since the only place known to host life in the Universe is a planet, i.e., the Earth, the detection and characterization of these objects is potentially the most promising path toward the answers to some of the most exciting and intriguing questions of mankind: "Are we alone in the Universe?", "How did life originate in the first place?" and "Are the Earth and the Solar System unique, or are they common in our galaxy?". The highly-improved capabilities of spectrometers of future astronomical facilities (e.g. ELT, JWST) will allow us to characterize the chemical composition of exoplanetary atmospheres. The detection of particular chemical elements (the so-called "bio-markers") in the atmospheres of terrestrial planets inside the habitable zone of their host star would provide strong indication for the presence of extra-terrestrial life in those systems. Even now, huge steps towards the understanding of exoplanets are already being made.

Since the discovery of the first exoplanet around a millisecond pulsar in the early 1990s (PSR1257+12, Wolszczan and Frail, 1992), and around a Solar-type star three years later (51 Peg b, Mayor and Queloz, 1995), more than 4000 new exoplanets have been found in almost 3000 planetary systems, mostly thanks to the *Kepler* space telescope (e.g., Borucki et al., 2011a,b). Not only is this a demonstration of the extraordinary technological advancements in the field of observational astronomy, but the ever-growing number of discovered exoplanets is revealing an unexpected and surprising variety of orbital properties and planetary masses (Winn and Fabrycky, 2015). This characteristic of the observed exoplanets is an indication that the planet formation process may lead to a wide variety of results.

Although understanding the origin of Earth has always been one of the overarching questions of science, many important aspects of the planet formation process are still far from being understood. This is not entirely surprising,

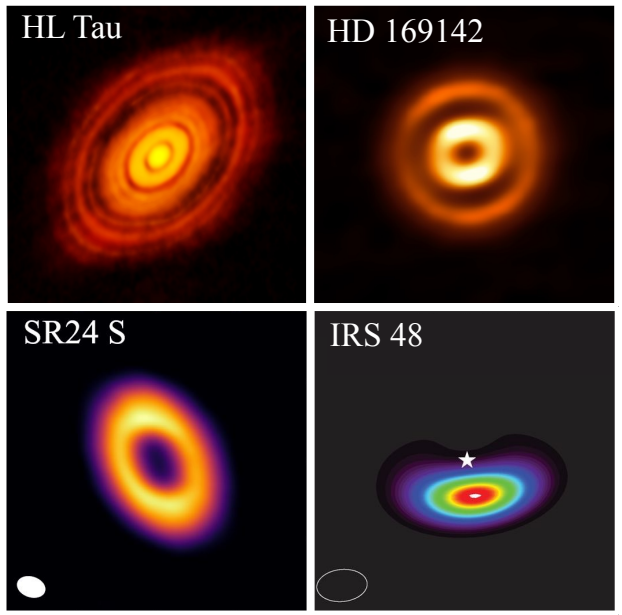


**Figure 1.1:** A few examples of early ALMA images of protoplanetary disks, showing an unexpected variety of rings, gaps and asymmetries, suggesting the presence of planets. Images from van der Marel et al. (2013), ALMA Partnership et al. (2015), Fedele et al. (2017), and Pinilla et al. (2017), from top-left to bottom-right.

considering the huge dynamical range involved in the making of a planet: the growth process from tiny sub-$\mu$m-sized dust particles such as those found in the interstellar medium (ISM) to full planets covers 13 orders of magnitude in size and about 40 in mass, and therefore involves many different physical processes (see Sec. 1.1.2). Moreover, the environments in which this growth occurs, called "protoplanetary disks", are also very complex because of the steep gradients in their properties and of the many physical and chemical processes shaping them. The study and understanding of protoplanetary disks and their evolution is therefore one of the pivotal aspects required to grasp the origin of planets and planetary systems, and ultimately the origin of life itself.

In recent years, the Atacama Large Millimeter/sub-millimeter Array (ALMA) has allowed an incredible breakthrough in the understanding of protoplanetary disks. Its unprecedented sensitivity, spatial and spectral resolution are allowing us to clearly observe the properties of the gaseous and mm-sized dusty components of these objects in details never imagined before (Fig. 1.1). Alongside ALMA, other new instruments such as VLT/SPHERE are allowing us to probe the smaller $\mu$m-sized grains, completing our already rich vision of proto-

planetary disks. In the meantime, the astrometric measurements of *Gaia* have mapped the 3D structure of our galaxy with a precision 200 times better than that of its predecessor *Hipparcos*, allowing us to calculate the distances of all the studied objects and nearby star forming regions with exquisite precision. Many questions are being answered, and many more arise: we are truly living in the Golden Age of observational planet formation!

This thesis will exploit the capabilities of these new instruments to study the gas and dust substructures observed in protoplanetary disks. The origin of these substructures can shed new light on the processes leading to the formation of planets, and help us understand what processes shape the observed exoplanetary systems.

## 1.1 Star and Planet formation

### 1.1.1 From clouds to stars

The path toward protoplanetary disks and, eventually, of planets, starts from molecular clouds, which are agglomerations of mainly molecular hydrogen gas and small sub-$\mu$m-sized dust grains, in a mass ratio of 100 to 1. Their typical masses are $10^2 - 10^5\,M_\odot$, with sizes up to hundreds of parsecs, temperatures between $\sim$ 10 to 100 K and densities of $10^2 - 10^4$ particles·cm$^{-3}$. At these temperatures and densities, thermal pressure is not enough to balance the gravitational force, and molecular clouds start collapsing undergoing the so-called Jeans instability, unless they are supported by some non-thermal pressure provided by turbulence, magnetic fields, or both. As they collapse, smaller and smaller regions become unstable, and the cloud fragments in a number of cores which ultimately lead to the creation of a cluster of individual protostars (e.g., Terebey et al., 1984; Shu et al., 1987; Galli and Shu, 1993).

If these cores possess even a small amount of angular momentum, their angular velocity increases during the collapse in order to conserve it. At some sufficiently small radius, the centrifugal force prevents the material in the collapsing clump from falling in a purely radial direction, giving rise to a flat, disk-shaped structure rotating around a newly formed protostar. Turbulence in the disks (Shakura and Sunyaev, 1973a), and possibly also self-gravity, winds and magnetic fields, cause a redistribution of angular momentum and a radial spread of the disk material (Armitage, 2011). In particular, some material loses angular momentum thus drifting inward accreting onto the star, whereas part moves outward to conserve angular momentum.

This evolutionary sequence is reflected in a classification of young stellar

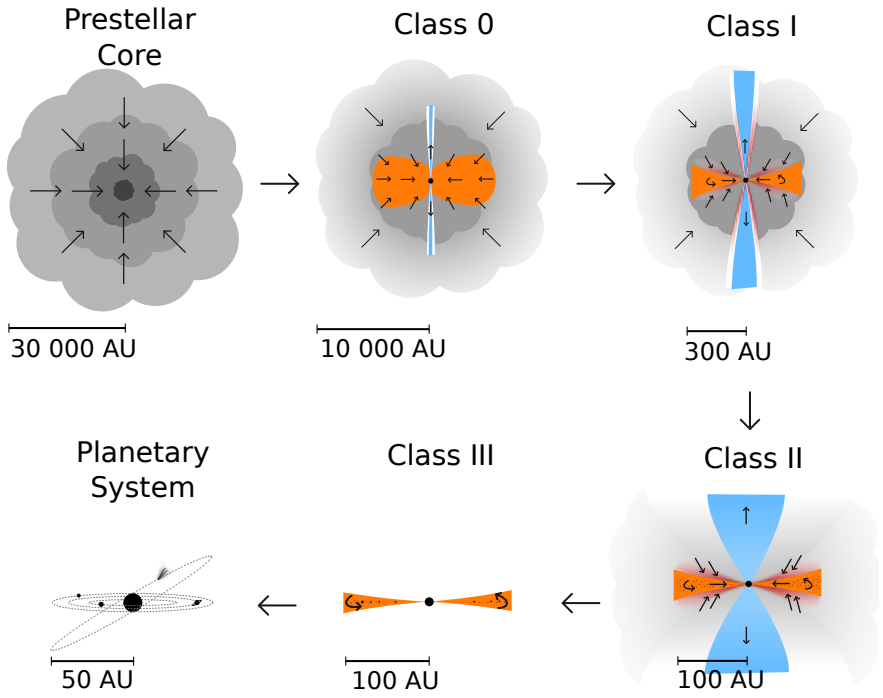


**Figure 1.2:** Representation of the evolution from prestellar core to planetary system, through the different classes of the protoplanetary disk phase. This thesis focuses on the Class II phase and on its transition to Class III. Figure by Magnus Persson.

objects (YSOs) based on the spectral slope of their spectral energy distribution typically in the 2.2 $\mu$m−20 $\mu$m wavelength range (Lada, 1987; Andre et al., 1993; Greene et al., 1994), and is represented in Fig. 1.2. Class 0 YSOs represent the earliest stages of the formation of a protostar, when it is still heavily embedded in its envelope which dominates the emission. As the envelope starts to be dissipated, emission from the central star as well as from the disk can be identified, and YSOs evolve into the Class I stage. When the Class II stage is reached, the envelope has completely dissipated; the central protostar is optically visible and surrounded by a protoplanetary disk which is optically thick in the infrared (IR) and mostly optically thin at mm wavelengths. Finally, Class III disks are even more evolved YSOs, where almost all the gas is dissipated and the star is surrounded by a planetary system and/or a "debris disk" made of asteroids and comet-sized objects, as well as smaller dust particles generated by the impact between the larger solid bodies.

This thesis will focus on the Class II evolutionary stage, where the capabilities of ALMA allow us to probe with unprecedented sensitivity and resolution the bulk of the dust content and the molecular emission from the gas (see Sec. 1.2.2). The transition from Class II to Class III stage will also be a topic of study.

### 1.1.2 From dust to planets

In the currently most widely accepted scenario, planets are formed in disks through the growth of microscopic dust grains that are found in the ISM. This growth process can be divided in different steps, depending on the physical mechanism driving this growth.

In the very first steps, tiny $\mu$m-sized dust grains grow in size by sticking after collision with other grains. Gravity is not important at these stages, and sticking can be explained by short-range van der Waals interaction. This can only happen for velocities $\lesssim 1 - 10\,\mathrm{m\,s^{-1}}$ (e.g., Dominik and Tielens, 1997; Blum, 2018); at higher velocities, sticking becomes less and less important, and the grains tend to fragment upon collision. At these small sizes, the dynamics of dust grains are still very well coupled to that of the gas, and their relative velocities depend on a number of factors such as turbulent mixing, Brownian motion, vertical settling and radial drift. Moreover, the stickiness of the dust grains also depends on other factors such as grain composition, ice mantles and fluffiness or shape. All of these factors should be considered when modelling dust growth (Brauer et al., 2008; Birnstiel et al., 2010).

The above processes produce the mm-sized particles that can be observed with ALMA, but larger cm-sized pebbles or even meter-sized bodies are also formed. At these radii and masses, however, the dynamical interaction between gas and dust begins to change, posing the first big problem along the path toward planet formation. Because of gas pressure that helps to counteract gravity, gas rotates around the central protostar at a slightly sub-Keplerian velocity. Tiny $\mu$m-sized grains are well coupled to the gas and feel this same pressure, but mm and meter-sized grains are more decoupled and are not supported by pressure. Consequently, they orbit at Keplerian velocity, i.e., slightly faster than the gas. This results in a headwind causing mm, cm and meter-sized grains to drift toward the central star on timescales as short as 100 years (Whipple, 1972; Weidenschilling, 1977), without having the time to grow to the size of planets. This barrier can be overcome because of the presence of regions where dust grains get trapped while drifting in the radial direction (Pinilla et al., 2012a,b, also see Sec. 1.3.1). In these "dust traps", grains have time to grow to larger sizes and to form the so-called planetesimals, with sizes of $1 - 100\,\mathrm{km}$.

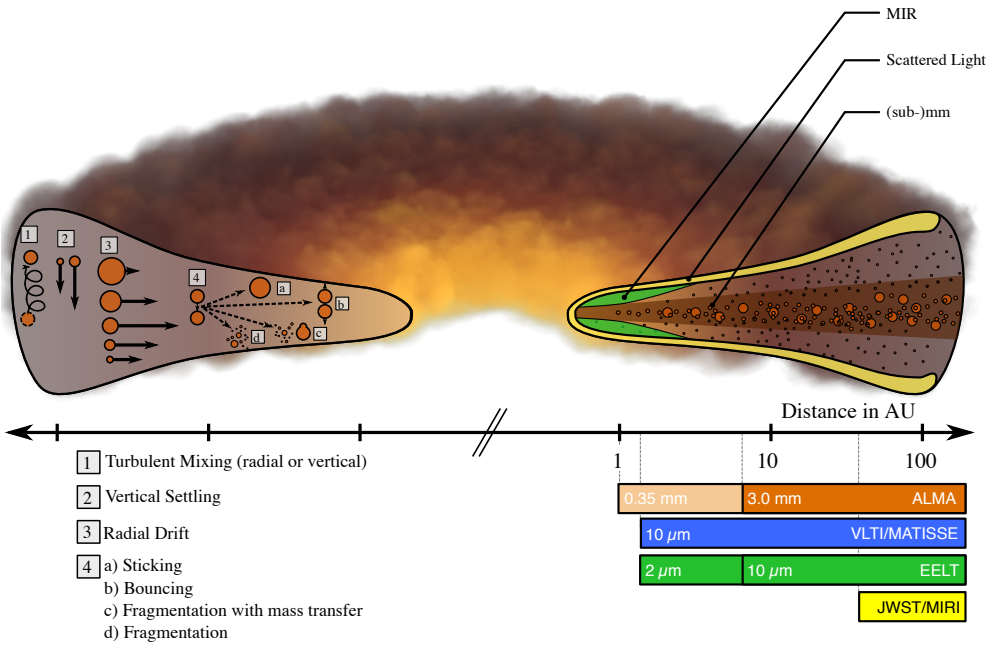


**Figure 1.3:** *Left-hand side:* Illustration of the relevant dust grain evolution processes leading to planet formation. *Right-hand side:* The left edge of the bars show the highest angular resolutions achievable with present and future observational facilities at different wavelengths and resolutions, assuming the typical distance of a nearby star-forming region (i.e., 150 pc). Figure from Testi et al. (2014)

These dust traps form ring-shaped structures in disks, as those observed from the very beginning with ALMA (see Fig. 1.1).

Once a population of planetesimals has been formed, gravity starts to dominate over sticking. At this stage rocky planets are formed, along with the cores of giant planets, which in turn form via gas capture.

## 1.2 Disk observations

Observational evidence of the presence of gas and dust around young stars exists for many years from a variety of different tracers, like optical emission spectra (Herbig, 1950), emission excess at IR wavelengths (Ney et al., 1973), and sub-mm continuum (e.g., Beckwith et al., 1990). However, it was not until the 1990s that the morphology of protoplanetary disks could really be determined. Optical high resolution observations with the *Hubble Space Telescope* (O'dell and Wen, 1994; O'dell and Wong, 1996), and in the mm with the IRAM Plateau

the Bure Interferometer (Dutrey et al., 1996), now called NOEMA, and later with SMA (e.g. Andrews and Williams, 2007) and CARMA (e.g. Isella et al., 2010) revealed flattened structures that were interpreted as disks projected on the plane of the sky (also see Sargent and Beckwith, 1991; Beckwith and Sargent, 1996). In some cases, observations of molecular lines, and especially of the CO rotational transitions observed in the mm showed velocity gradients along the major axis of disks, interpreted as evidence of material in Keplerian rotation around the central young star (e.g., Koerner et al., 1993; Simon et al., 2000). It is only in the last years, however, that we were able to really capture the structure of protoplanetary disks, after the advent of the most powerful mm-wavelength telescope ever.

### 1.2.1 ALMA

The Atacama Large Millemeter/submillimeter Array (ALMA) is an interferometer located on the Chajnantor plateau, in the Chilean Andes, at an altitude of about 5000 m above sea level, and its advent in 2011 marks one of the most important milestones in the history of the study of star and planet formation. ALMA is a partnership of ESO (representing its member states), NSF (USA) and NINS (Japan), together with NRC (Canada) and NSC and ASIAA (Taiwan) and KASI (Republic of Korea), in cooperation with the Republic of Chile.

It is an array of 66 antennas operating in 10 different Bands at wavelengths between 0.3 mm and 3.6 mm (see Tab. 1.1). Its main array has fifty 12 m antennas. An additional compact array of four 12 m antennas, and twelve 7 m antennas complement it. The antennas can be arranged in different configura-

**Figure 1.4:** Some of the 12 m antennas of the Atacama Large Millemeter/submillimeter Array (ALMA). Picture from ESO/B. Tafreshi

tions, where the maximum distance between antennas, called a "baseline", can vary between 150 m and 16 km. ALMA is an interferometer: it samples the Fourier-transform of the sky emission on a range of scales corresponding to the baselines between antennas. These samples can be used to estimate the sky brightness with a resolution corresponding to the (approximately) the longest sampled baselines. In the case of ALMA, this translates into a resolution of the order of the milli-arcsec (mas). The diameter and number of antennas, finally, provide it with a collecting area of 6492 $m^2$, resulting in a level of sensitivity that allows to observe targets in a fraction of the integration time of previous generation interferometers.

These unique features allow us to carry out resolved observations of hundreds of disks, as well as to resolve substructures in them in both dust and gas. As a result, surveys of populations of protoplanetary disks in different star forming regions, encompassing different ages and environments, are now being performed, allowing for observational tests of evolutionary theories and theoretical predictions.

### 1.2.2 Dust observations

Mm and sub-mm wavelengths, i.e. ALMA's observation wavelengths, are particularly well suited for the observation of protoplanetary disks as they allow us to probe the bulk of the solid material that disks are made of. The reason for this is twofold.

**Table 1.1:** ALMA Bands and relative observing wavelength/frequency range

| Band | Wavelength [mm] | Frequency [GHz] |
|---|---|---|
| 1⋆ | 6-8.5 | 35-50 |
| 2⋆ | 3.3-4.5 | 65-90 |
| 3 | 2.6-3.6 | 84-116 |
| 4 | 1.8-2.4 | 125-163 |
| 5 | 1.4-1.8 | 163-211 |
| 6 | 1.1-1.4 | 211-275 |
| 7 | 0.8-1.1 | 275-373 |
| 8 | 0.6-0.8 | 385-500 |
| 9 | 0.4-0.5 | 602-720 |
| 10 | 0.3-0.4 | 787-950 |

⋆ Not installed at the time of writing

First, the thermal radiation emitted by cold (10-50 K) dust particles depends on the particle size. In particular, the emission at a wavelength $\lambda_{\rm obs}$ is dominated by the emission of grains with size comparable to $\lambda_{\rm obs}$ (Draine, 2006). Therefore, protoplanetary disks are expected to be the brightest at mm-wavelengths, since theoretically the dust population of Class II protoplanetary disks is mostly made of mm-sized grains, as explained in Sec. 1.1.2. Observationally, evidence for the presence of large grains in protoplanetary disks can be obtained by measuring the spectral index $\alpha_{\rm mm}$, which depends on the maximum grain size: values of $\alpha_{\rm mm}$ lower than 3 in protoplanetary disks are regularly measured and are interpreted as a sign of the presence of large, mm/cm-sized grains (e.g., Ricci et al., 2010b,a; Testi et al., 2014).

The second reason that makes mm-wavelengths particularly interesting when observing protoplanetary disks, is the fact that at these wavelengths the emission is expected to be optically thin. This means that the total measured flux $F_\nu$ at a frequency $\nu$ is proportional to the dust mass through the relation

$$F_\nu = \frac{B_\nu(T)}{d^2} k_\nu M_{\rm dust}, \tag{1.1}$$

where $B_\nu$ is the Planck function at temperature $T$, $d$ is the distance, $k_\nu$ is the dust opacity at frequency $\nu$ and $M_{\rm dust}$ is the dust mass of the disk. At mm-wavelength, $k_\nu$ scales with frequency as $k_\nu \propto \alpha$, and $F_\nu^\beta$ is well represented by the Rayleigh-Jeans approximation:

$$F_\nu \sim T k_\nu M_{\rm dust} \nu^{\alpha_{\rm mm}}, \tag{1.2}$$

where $\alpha_{\rm mm} = 2 + \beta$. This also means that the radiation emitted by grains located deep below the surface of the disk is not reabsorbed, and therefore that mm observations can probe dust grains close to the midplane, where planet formation occurs.

The shorter the observing wavelength, the more optically thick the radiation becomes. In ALMA Band 9 and 10, between 0.3 and 0.5 mm, the disk emission is mostly optically thick in the inner tens of au, and even more so at higher frequencies in the optical/near-IR. At these wavelengths, the radiation from the central star is efficiently scattered from the small, $\mu$m-sized dust grains. Optical images at high angular resolution can then be used to investigate the geometrical structure of the disk surface layers. VLT/SPHERE allows now for $<0.1''$ resolution observations, and have revealed in the last years a variety of substructures such as rings (Ginski et al., 2016; van Boekel et al., 2017) and spiral arms (Benisty et al., 2015, 2017; Stolker et al., 2016).

A combination of observations at short and long wavelengths has the potential to cast light on the distribution of dust grains of different sizes and

at different depth into the disks. This is critical to test our expectations and theoretical predictions about gas/dust interaction and to understand the mechanisms creating the dust substructures.

### 1.2.3 Gas observations

Part of the mm radiation coming from protoplanetary disks is not due to the dust, but rather to the rotational line emission of gaseous molecules. Albeit 100 times more abundant than dust, gas is much more elusive to observe. The main reason for this is the fact that the most abundant molecule, $H_2$, possesses no dipole moment. The second most abundant molecule is CO, which in the ISM is 10000 times less abundant than $H_2$, although some studies suggest that in disks it might actually be even less abundant (Bergin et al., 2013; Miotello et al., 2017).

The interpretation of gas emission is far less trivial than that of the dust. Molecular emission not only depends on the overall gas density, but also on the

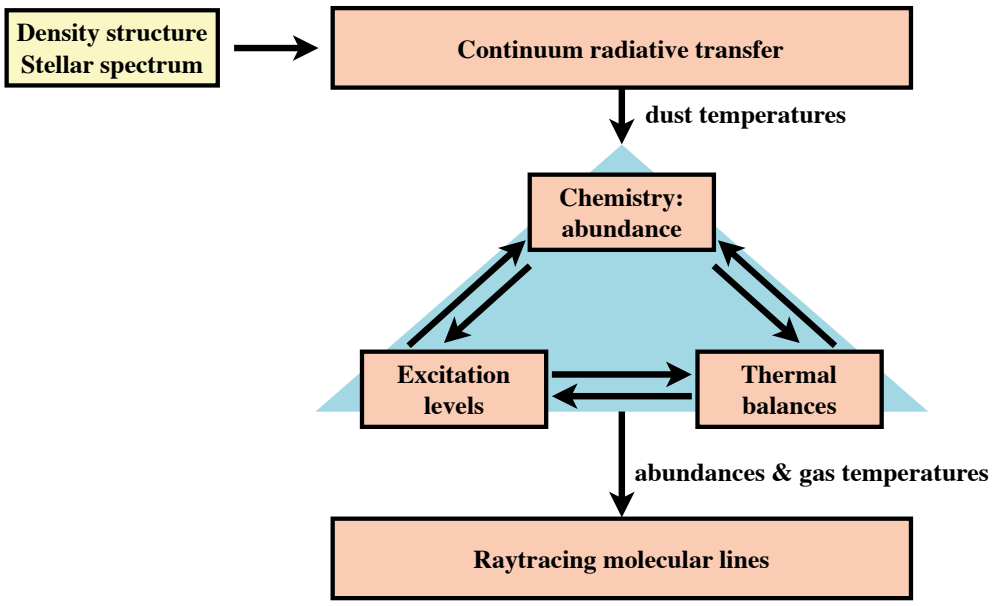


**Figure 1.5:** Diagram illustrating the DALI modelling procedure. After a density structure and a stellar spectrum are given as inputs, the dust temperature is estimated using continuum radiative transfer. The molecular abundances and gas temperature are then calculated self-consistently, and simulated observations are finally produced as outputs.

abundance of the molecule being observed with respect to the overall gas content. The abundance is regulated by a number of chemical reactions depending on many different physical properties of the disk. For example, the radiation field causes molecules to photo-dissociate and ionize, the dust temperature affects molecular freeze out, and the gas temperature and density affect the rate of the chemical reactions and the molecular excitation. In turn, the cooling rate of the gas, and therefore the gas temperature, depends on the molecular abundances and excitations. To make things even more complicated, in a protoplanetary disk all these physical parameters can vary with very steep gradients.

In order to take all of the above factors into consideration simultaneously, and therefore to be able to interpret gas observations in disks and to link them to the disks' physical properties, detailed physical-chemical modelling is required. The code used in this thesis is DALI (Dust And LInes, Bruderer et al., 2012; Bruderer, 2013). Assuming a given axisymmetric density structure and stellar radiation field the DALI modelling procedure is as follows (see Fig. 1.5):

1. The dust temperature is calculated through a Monte Carlo radiative transfer method.

2. Using an initial guess for the gas temperature, the chemical abundances for the different molecular species are calculated, along with the molecular excitations.

3. Based on the new abundances and excitations, the heating/cooling rates are updated.

4. The gas temperature is updated solving heating=cooling.

5. Steps 2 to 4 are repeated until convergence.

6. Based on the molecular excitations and abundances, a synthetic observation can be ray-traced,

The most relevant chemical reactions and rates used for the abundance and temperature calculations are included in a chemical network. In recent years, DALI has been used to model in great detail the emission of CO and of its isotopologs ($^{13}$CO and C$^{18}$O) in full and transitional disks[1] (Miotello et al., 2014; van der Marel et al., 2016a), as well as to study the dependence of other molecular line observations on disk's physical parameters (e.g., Bruderer et al., 2015; Kama et al., 2016; Trapman et al., 2017; Visser et al., 2018; van Terwisga

[1]Disks with an inner dust cavity

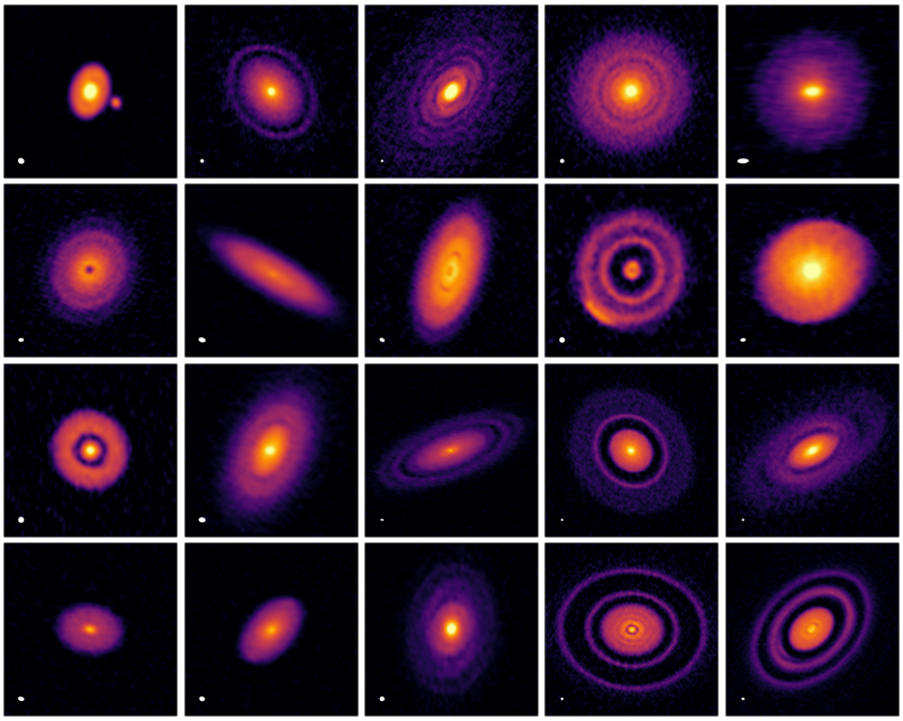

**Figure 1.6:** Overview of the high-resolution observations from the ALMA DSHARP large program (Andrews et al., 2018, and references therein). All of the observed disks clearly shows some substructures.

et al., 2019). In this thesis, DALI is used to model CN emission and morphology in protoplanetary disks. After CO, CN has often the brightest lines in disks, with intensities comparable to those of $^{13}$CO but tracing layers higher up in the disk, being more sensitive to the UV photoprocesses.

## 1.3 Disk sub-structures

### 1.3.1 Structures in the dust

From the early observations of protoplanetary disks with ALMA, shown in Fig. 1.1, it has become clear that disks are not the smooth and axisymmetric structures imagined in the 90s and early 2000s. Each new high-resolution observation is rather showing us that almost every single disk hosts at least some kind of sub-structure, be them rings, vortices, cavities, or spiral arms.

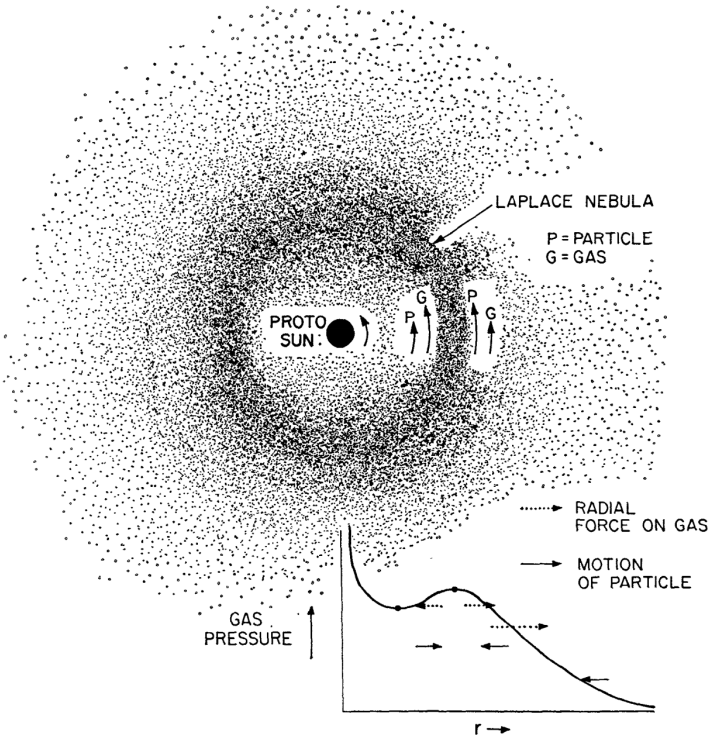


**Figure 1.7:** Radial pressure maxima in protoplanetary disks produce dust traps, that result in accumulations of mm-sized dust grains. When observed with ALMA, these can appear as rings. Figure from Whipple (1972).

This scenario has been strengthened by the first ALMA large program on protoplanetary disks (DSHARP Andrews et al., 2018, Fig. 1.6).

From the very beginning, planets have been invoked as the most natural explanation for these structures (e.g., Dipierro et al., 2015a). Assuming that a planet formed in a disk, the tidal forces would subtract angular momentum from the material orbiting inside the planet's orbit and redistribute it to the material at larger radii. This type of interaction would then carve a gap in the gaseous disk, accumulate material at the edges of the gap and produce local maxima in the gas pressure radial profile. As noted in Sec. 1.1.2 and as shown in Fig. 1.7, these pressure maxima act like dust-traps, preventing mm-sized dust grains from radially drifting into the star and instead accumulating them in ring-shaped structures such as those observed with ALMA. Moreover, when

the planet is very massive and orbiting at small radii or in the case of a binary, an entire cavity can be cleared and a hole in the inner region of the hosting disk can be created, thus originating a transitional disk (e.g., van der Marel et al., 2016a).

The interaction between a massive planet and a disk does not only create gaps and rings but can also result in spiral arms (e.g., Dong et al., 2015a; Stolker et al., 2016), or trigger the Rossby-Wave instability (Lovelace et al., 1999; Li et al., 2000, 2001) giving rise to high-pressure regions called vortices that can trap dust azimuthally and form crescent-shaped dust asymmetries such as those observed at mm-wavelengths (Lyra et al., 2009; Lin, 2012; van der Marel et al., 2013). While spiral arms are mostly observed in scattered light, crescent-shaped structures are almost exclusively seen at mm-wavelengths. One of the aims of this thesis is to understand the relation between these two types of structures, and how the different dynamical couplings of dust grains with the gas play a role in this.

On the one hand these dust traps provide the solution for the meter-sized barrier and are the ideal environment for dust to grow up to planetesimal size, but it is nevertheless clear that they cannot be at the origin of the formation of all planets, as first-generation planets are still required in order for dust traps to be triggered. To make this problem even worse is the fact that, despite all the efforts and instrumentation built specifically for the purpose of imaging planets embedded in disks (e.g. VLT/SPHERE and the Gemini Planet Imager, GPI), only one such planet has so far been imaged (PDS 70b Keppler et al., 2018). A handful additional planets have been proposed on the basis of indirect evidence in the gas kinematics (e.g., Pinte et al., 2018, 2019; Teague et al., 2018).

It is therefore becoming more and more clear that not all of these structures can be due to massive planets, and that some additional explanations are required in order to really answer the question about how planets form.

### 1.3.2 Structures in the gas

If the structures observed in the dust emission can be directly interpreted in terms of dust distribution, gas structures are harder to interpret because of the interplay between gas density, temperature, and chemistry regulating molecular abundances and their excitation, and ultimately regulating their gas emission (see Sec. 1.2.3). Because different molecular species form and emit under different conditions, when properly modelled the structures in the gas can provide unique information about the physical properties of the disks (see Fig. 1.8).

Rings have been observed in $N_2H^+$ (Qi et al., 2013): since this molecule can only be present in large abundance where CO is frozen-out onto the grains,

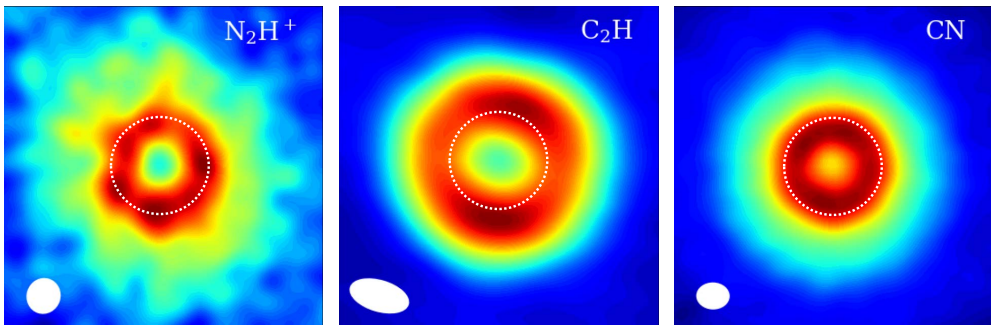


**Figure 1.8:** Emission detected in the TW Hya disk($d$=60 pc) coming from 3 different molecular species. All three molecules show annulus-like structures, but the inner and outer radii of the annuli are different in each species. This illustrates how the emission from different species traces different physical and chemical conditions. The dotted circle has a radius of 1″ (60 au). Data from Bergin et al. (2013), Qi et al. (2013), and Teague et al. (2016).

the location of the $N_2H^+$ ring is thought to trace the CO "snowline". At larger radii, the temperature is too cold for CO to survive in its gaseous state; at smaller radii, the warmer temperature allows CO to desorb from the dust grains. A double ring has been observed in $DCO^+$ (Öberg et al., 2015): the inner one can be explained by the same mechanism as above; the outer one, however, can only be explained by non-thermal desorption of CO from the dust grains. This happens because the column densities at these large radii are low enough to allow UV photons from the central star and the ISM to penetrate down to the disk midplane, hitting the grains and desorbing CO molecules. Alternatively, this second desorption front could be explained by an increasing dust temperature at large radii: this happens because the dust grains, on average smaller in size at large radii, are more easily stirred up by turbulence, thus intercepting more of the stellar radiation and finally heating-up (Facchini et al., 2017).

Lastly, hydrocarbon rings in $C_2H$ and c-$C_3H_2$ have also been observed (Bergin et al., 2016). Such bright rings are due to a combination of high UV fluxes in the upper layers of the disks, and a combination of CO and $H_2O$ freeze-out leaving the outer disk depleted in both C and O, but with an overall C/O>1 (Öberg et al., 2011). As a consequence, not all of the C will end up into CO, but some will be left free to form hydrocarbons.

Even more recently, CN rings have been observed in TW Hya (Teague et al., 2016), and in two disks in the Lupus star-forming region, namely Sz 71 and Sz 98 (van Terwisga et al., 2019). Proper modelling is required to understand under

which conditions CN emission can be ring-shaped, and which information CN rings can provide about the physical and chemical structures of protoplanetary disks.

## 1.4 SPH hydrodynamical models

In this thesis, hydrodynamical simulations were performed using the `PHANTOM` Smoothed Particle Hydrodynamics (SPH) code (Lodato and Price, 2010; Price and Federrath, 2010). The SPH method is a Lagrangian hydrodynamical scheme originally formulated by Lucy (1977) and Gingold and Monaghan (1977). A Lagrangian formulation of the fluid equations considers the evolution of the fluid properties for any given fluid element, whose position is in general not constant. This is different from the Eulerian approach, where the evolution of the fluid variables is followed in a given point in space. Eulerian numerical methods therefore use geometric grids, either fixed or adaptive, and are called grid-based codes. Lagrangian formulations such as SPH, rather than discretising space in cells, discretise the fluid quantities into particles of fixed mass, moving with the fluid velocity.

In SPH a continuous density distribution is then computed using the kernel weighted sum

$$\rho(\mathbf{r}) = \sum_{b=1}^{N_{\rm part}} m_b W(|\mathbf{r} - \mathbf{r}_b|, h), \tag{1.3}$$

where $W$ is a function called the "smoothing kernel", and should be positively defined, monotonically decreasing with distance and isotropic. The simplest example of $W$ is a 3D Gaussian. $h$ is called "smoothing length" and is in general $h = n(\mathbf{r})^{-1/3}$: this way, the smoothing length (and the resolution) follows the number density.

The density calculation is the key aspect of SPH and immediately shows some of its advantages. First the resolution of the method will follow the mass, since each particle carries a fixed mass and therefore density can only increase due to a higher concentration of particles. This is particularly well suited for astronomical problems involving gravitational collapse, since the dense regions will be better resolved. Second, since particles cannot lose, gain or diffuse mass, it will be an exactly conserved quantity.

Once the density distribution is calculated with Eq. 1.3, the Lagrangian (i.e., the difference between kinetic and potential energy) can be calculated. Combining the Lagrangian and the relative Euler-Lagrange equation with the first law of thermodynamics and the gradient of the density in Eq. 1.3, the

equations of motions can finally be derived self-consistently.

From this approach follow some other key features of SPH. The derivation of the equations of motion from the Lagrangian implies that the symmetries in the Lagrangian will reflect into conservation properties in the equations of motions. In particular, when the right smoothing kernel is chosen, linear and angular momentum, energy and entropy are exactly conserved, in addition to mass. This also means that the intrinsic dissipation in SPH is zero, i.e., that viscosity should be added manually when needed. This is sometimes necessary, e.g. to deal with shocks: ironically, this makes SPH codes intrinsically more dissipative than grid codes, and not well suited for the studies of disks in conditions of very low viscosity.

More details on the SPH code and on its advantages and disadvantages with respect to grid-based codes can be found in Price (2012).

## 1.5 This thesis and future outlook

ALMA and VLT/SPHERE have opened, since the beginning of this PhD work, a whole new branch within the field of planet-formation: the study and interpretation of substructures in protoplanetary (potentially planet-forming) disks. ALMA detected and spatially resolved substructures in both gas and mm-sized dust. SPHERE observed additional structures in $\mu$m-sized dust, linked to the gas. The fact that gas and solids of different sizes have different dynamics is now undisputed, but a clear connection between the structures observed with the different tracers is still missing. Are all substructures due to planets that have already formed in the disks? How many planets are needed to explain them? Or are they the signpost of ongoing planet formation? A comprehensive answer to these questions can only be provided by simultaneously explaining the substructures in the gas and dust at different wavelengths.

- In Chapter 2 the GG Tau ($d$=140 pc) circumbinary disk is studied in detail. Hydrodynamical simulations coupled to dust evolution models are carried out in order to model the system and reproduce archival observations in both gas and mm-sized dust simultaneously. The analysis allows to put strong constraints on the binary orbit. In particular, in order to reproduce the gas cavity size and the location of the dust ring observed at mm-wavelengths, the binary orbital plane and that of the protoplanetary disk must be misaligned with respect to each other.

- In Chapter 3, new ALMA Band 7 (0.8 mm) observations of the disk around HD 135344B ($d$=135 pc) are presented. Thanks to the new $0''.2$

($\sim$ 30 au) resolution achieved, this disk, which in previous observations appeared as a single slightly asymmetric ring, is now resolved into an inner, symmetrical ring and an outer asymmetric structure. A fit of the image shows that the asymmetry is consistent with a vortex. The images at mm-wavelength have also been compared to the scattered light observations, showing "grand-design" (two-armed) spiral arms. A scenario explaining both the mm-dust structures and the $\mu$m-dust ones is proposed. In this scenario, the spiral arms are launched by the vortex itself, and a single planet is needed to explain all the structures, rather than 2 or 3 planets as in previous interpretations (e.g., Stolker et al., 2017).

- Chapter 4 presents new very high resolution ($0''.06$, $\sim$ 10 au) ALMA Band 3 (3 mm) and Band 4 (2 mm) observations, requested in order to test the scenario proposed in Chapter 3. A multi-wavelength analysis is then performed by combining these observation with our Band 7 and archival Band 9 observations. With this analysis, different theoretical predictions of dust dynamics and evolution inside a vortex were tested, thus allowing to confirm the nature of the HD 135344B asymmetry as a dust-trapping vortex. Most notably, a shift in the peak of the emission of the vortex, due to different dust distributions of grains of different sizes, was measured for the first time. The mass of the vortex was also calculated, and was found to be high enough to launch spiral arms, as proposed in van der Marel et al., 2016b.

- In Chapter 5, CN emission in protoplanetary disks is modelled in detail using the thermo-chemical code DALI. The main result is that CN emission is always ring-shaped, independently of the underlying dust structure. The size of the rings and their brightness can provide information about the flaring of the disk, the UV flux from the central star, as well as the disk size.

- In Chapter 6, a survey of protoplanetary disks in the Corona Australis (CrA, d=154 pc) star forming region with ALMA Band 6 (1.3 mm) is presented. The disks in CrA appear very different from those in other regions of the same age previously surveyed. The measured fluxes are lower than expected, and the disks are smaller and do not show any substructure. Different possible explanation for are explored: it is possible that two different star formation events, a few Myrs apart, have occurred, with the older population already on its way to its Class III stage; alternatively, the initial conditions at the epoch of star formation may play a role in the properties we observe today.

The main conclusions of this thesis are the following:

1. The size of the dust ring around the GG Tau binary can only be explained if the orbital plane of the binary is misaligned with respect to the disk.

2. The spiral arms observed in scattered light may be triggered by massive vortices rather than by planets. This scenario can explain the structures observed in HD 135344B.

3. CN emission is ring-shaped even in full disks, with its location unrelated to that of any dust ring. The ring size and flux can provide information about the physical structure of the disk.

4. The mm-fluxes of the Class II disks in the CrA star forming region are lower than expected in a region of its age, and their dust radii are smaller. This could be due to the initial conditions of the star forming process, or to an old stellar population in the CrA region alongside the young one.

To date, it remains unclear whether the observed structures are due to already formed planets or to some other physical mechanism. So far only one planet has been imaged in a disk (Keppler et al., 2018), but future observations may directly image more embedded planets associated with these structures. In the meantime, new promising approaches to indirectly infer the presence of planets are becoming more and more common and will prove critical in the near future. The perturbations to the gas kinematics induced by planets, for example, has already been used in a few cases (e.g., Pinte et al., 2018; Teague et al., 2018), and the same technique can now be applied for more systems. Emission from circumplanetary disks associated to embedded protoplanets (Isella et al., 2019; Pérez et al., 2019) as well as the emission associated to their accretion onto the planets (Haffert et al., 2019) have also recently been detected with ALMA and MUSE, respectively. Such observations may be more common in the future.

In the meantime, additional multi-wavelength studies of protoplanetary disks such as that carried out for HD 135344B can shed light on the dust properties inside dust traps, including inside vortices. In particular, the connection between vortices in the mm and spiral arms in scattered light should be better investigated in more systems (e.g. V1247 Ori and MWC 758), also exploiting the sensitivity and spatial resolution of ALMA at the high frequencies available in Band 9 and Band 10.

These studies are critical to understand if substructures in disks are the birthplace of new planets. They will ultimately also tell whether and how the variety of structures observed at mm-wavelengths is linked to the diversity in the exoplanetary systems' properties.